1

2

3 **Adaptation of peristaltic pumps for laminar flow experiments**

4

5 Javier Abello[1], Yvette Y. Yien[2], and Amber N. Stratman[1,+]

6

7

8 1. Department of Cell Biology and Physiology, Washington University in St. Louis School of

9 Medicine, St. Louis, MO 63110

10 2. Pittsburgh Heart, Lung and Blood Vascular Medicine Institute and Department of

11 Medicine, University of Pittsburgh, Pittsburgh, PA 15261

12

13

14

15

16

17

18 +Correspondence: a.stratman@wustl.edu (ANS)

19 **Key Words**: laminar flow, pulsatile flow, endothelial cells, in vitro modeling

20

21

22

1

# Abstract

Endothelial cells (ECs) are the primary cellular constituent of blood vessels that are in direct contact with hemodynamic forces over the course of a lifetime. Throughout the body, vessels experience different types of blood flow patterns and rates that alter vascular architecture and cellular behavior. Because of the complexities of studying blood flow in an intact organism, particularly during development, modeling of blood flow *in vitro* has become a powerful technique for studying hemodynamic dependent signaling mechanisms in ECs. While commercial flow systems that recirculate fluids exist, many commercially available pumps are peristaltic and best model pulsatile flow conditions. However, there are many important *in vivo* situations in which ECs experience laminar flow conditions, such as along long, straight stretches of the vasculature. To understand EC function under these situations, it is important to be able to consistently model laminar flow conditions *in vitro*. Here, we outline a method to reliably adapt commercially available peristaltic pumps to reproducibly study laminar flow conditions. Our proof of concept study focuses on 2-dimensional (2D) models but could be further adapted to 3-dimensional (3D) environments to better model *in vivo* scenarios such as organ development. Our studies make significant inroads into solving technical challenges associated with flow modeling, and allow us to conduct functional studies towards understanding the mechanistic role of flow forces on vascular architecture, cellular behavior, and remodeling during a variety of physiological contexts.

## Introduction

41

42 Perfusing 2D or 3D cultures of endothelial cells (EC) with fluid is a popular technique to model

43 the effects of blood flow and shear stress forces on the vasculature [1-16]. *In vitro* systems have

44 been built to mimic individual types of flow forces or patterns felt by ECs along different regions

45 of the vascular tree, including oscillatory, pulsatile, and laminar. Consistent with what is observed

46 under physiological conditions, ECs cultured *in vitro* under laminar flow conditions align parallel

47 to the direction of flow [5, 6, 14-29]. Similarly, ECs experiencing pulsatile or oscillatory flow

48 conditions remain more haphazardly organized, or with a perpendicular alignment to the flow

49 direction [5, 6, 14, 15, 17-29].

50

51 While significant research has been done to build reliable platforms capable of generating

52 physiologic levels of laminar versus oscillatory/pulsatile flow forces, systems remain inaccessible

53 to the broad vascular biology research community for a number of reasons. For many, the price

54 of a full commercial system capable of altering flow patterns, rates, or flow type prevents use of

55 this modeling technique. Peristaltic pumps are more cost effective but best suited to mimic

56 pulsatory/oscillatory flow conditions, due to the design of the pump controlling the flow rates [30].

57 To account for this, we have adapted and optimized a commercially available, multi-head

58 peristaltic pump system that has its own controller software [31], to be able to reproducibly perform

59 laminar flow or pulsatile flow experiments (**Fig 1A**). Here, we will outline the steps needed to

60 create pulse dampeners from easy to access supplies, that can attach to a peristaltic pump to

61 generate laminar flow. Further, we discuss our parameters for eliciting flow responses,

62 standardization/validation of this pump system, and downstream analysis techniques for studying

63 cell biology using this platform.

64

## Results

65

**Generation of dampeners to offset pump pulsation**

66

67 Addition of a dampener to a peristaltic pump is one way to offset the pulsatile forces generated

68 by the mechanical properties of the pump. To do this, we utilized easy to access and cost-effective

69 supplies to custom make small footprint dampeners to attach to any flow system (**Fig 1B**). To

70 create the body of the dampener, the barrel of a 10 mL syringe (BD) was cut 12 mm from base of

71 the barrel. A thin wall polypropylene tube (Beckman) was bonded to the syringe barrel by applying

72 a thin layer of two-parts urethane adhesive (J-B Weld Company), following the manufacturer

73 recommendation. Because the internal diameter of the syringe barrel is 13.34 mm and the

74 external diameter of the polypropylene tube is 14.43 mm, to assemble the dampener body both

75 parts must be forced together, which along with the adhesive avoids air or liquid leaks. The tubing

76 connection to the dampener was created with 2.5 cm silicone tube (FisherBrand) inserted directly

77 to the syringe Luer-Lok tip. At the other end of the silicone tubing, a T-type connector (Nalgene)

78 was inserted (**Fig 1B**). Two dampeners are connected to the system, one on the inlet and one on

79 the outlet side of the system between the pump head and its respective media reservoir. The

80 dampeners must be vertically oriented to ensure proper function.

81

82 The media reservoirs were constructed using 30 mL high density polyethylene (HDPE) bottles

83 (Nalgene). Two holes 4 mm in diameter were drilled in the caps of the HDPE bottles and two

84 elbow luer connectors male (ibidi) were bounded to the caps using the two-parts urethane

85 adhesive described above. At the interior of the cap two pieces of 2 and 4 cm silicone tubing were

86 attached to the elbow connector as inlet and outlet ports respectively.

87

88 Efficacy of the generation of laminar flow was confirmed two ways. The first was done via real-

89 time visualization of Quantum dots (Qdots) within the circulating media (**Videos 1 and 2**). As

90 shown in the videos, without the dampener (**Video1**) there is a clear rhythmic stopping of the

4

91    fluid/Qdots as they transverse the flow chamber (flow is moving left to right across the video). This

92    pulsation is virtually eliminated after addition of dampeners (**Video 2**). To quantify the

93    effectiveness of the dampeners in offsetting the inherent pulsatile nature of the pump, we installed

94    a liquid flow sensor to the silicone tubing (Sensirion) enabling us to determine directionality of flow

95    (positive flow moving left to right across the sensor, negative if flow is moving right to left across

96    the sensor) and the dynamic liquid flow rates of the system (**Fig 2**). The sensor was installed

97    before the inlet attachment point of the µ-Slide | $^{0.4}$ Luer slide of the flow circuit (**Fig 2A**). The

98    system was evaluated under the following conditions: 1) the flow system without dampeners,

99    using the original function of the pump (pulsatile, **Fig 2A-C**); 2) the flow system modified with

100   dampeners installed at the inlet and outlet of the pump head (laminar, **Fig 2D-F**); and 3) the flow

101   system modified with a commercial dampener (Sensirion) installed before the sensor as is

102   recommended by the manufacturer (laminar, **Fig 2G-I**). The system was placed under our

103   standard experimental conditions (5% $CO_2$, 37°C, and 95% humidity for 24 hours), and 15 second

104   measurements of fluid flow taken at 1 and 24 hours. The two time points were chosen to

105   demonstrate the stability of flow forces across the time frame of experimentation. As shown, the

106   non-modified pump as purchased has a rhythmic pulsation to it (**Fig 2B**), that can be dramatically

107   off-set by the incorporation of dampeners into the flow circuit (**Fig 2E**). As a direct comparison,

108   we tested the performance of a commercial dampener, and demonstrate our homemade

109   dampeners were able to out preform a commercial version and suppress pulsation more

110   dramatically (**Fig 2E, H**). While there is still minimal pulsation within the system, it is reduced

111   approximately 6-fold, and reliably allows us to utilize this system to observe phenotypic

112   differences in endothelial cell behavior in response to variation in type of flow stimuli.

113

114   **Validation of cellular behavior in flow assays via live imaging analysis**

115   To confirm that altered cellular behaviors are generated in response to differing flow stimuli from

116   our modified pump system, we set up 2D live imaging assays to longitudinally track cellular motility

117   and alignment over a 24 hour period. Human umbilical vein endothelial cells (HUVECs) or human

118   aortic endothelial cells (HAECs) were grown to confluence (2.5 x $10^5$ cell/slide) on 1mg/ml gelatin

119   coated μ-Slide | $^{0.4}$ Luer slides in 1x M199 media supplemented with 20% fetal bovine serum

120   (FBS), 25 μg/mL of Endothelial Cell Growth Supplement (ECGS), 0.01% heparin sodium salt, and

121   1x Antibiotic-Antimycotic at 5% $CO_2$, 37$^o$C, and 95% humidity. The slides were then acclimated

122   to a microscopy system containing a climate-controlled stage top incubator (EVOS M7000) to be

123   cultured under conditions of constant laminar flow, at 12-15 dynes/cm$^2$/sec, or constant pulsatile

124   flow, at 12-15 dynes/cm$^2$/sec and 60 RPM, for 24 hours. To help maintain cell health, at the start

125   of the experiment the rate of flow was stepwise increased 10% every 10 minutes until reaching

126   the desired final experimental flow rate.

127

128   Utilizing a microscope with a stage top incubator allows us to carry out multipoint, time-lapse

129   image acquisition. Images were acquired every 20 minutes for 24 hours to follow dynamic

130   changes in cell shape and alignment over time (**Videos 3 and 4, Fig 3A,B**). At the end of the

131   experiment, the individual images are assembled into a video file to watch cellular behavior across

132   the full 24 hours of imaging. Angle of alignment (**Fig 3C,D**), cellular tracking (**Fig 3E**), and total

133   distance moved/speed of motility (**Fig 3F,G**) amongst other features can be analyzed from these

134   videos utilizing free ImageJ/Fiji software [32]. Our results show that in response to laminar flow,

135   ECs align to and move against the direction of flow over the 24 hour imaging period (**Fig 3D,E,**

136   **Video 4**), while ECs subjected to pulsatile flow largely remain perpendicular to the direction of

137   flow and move in a more haphazard fashion over the 24 hour imaging period (**Fig 3C,E, Video**

138   **3**). Under both flow conditions, HUVECs on average move the same total distance and at the

139   same velocity (**Fig 3F,G**). This behavior mimics what is seen both *in vivo* and *in vitro* flow models

6

140     [5, 6, 14-29], validating that our system does indeed reliably model flow stimuli to elicit the

141     expected changes in cellular behavior.

142

143     From a practical standpoint, live imaging does not have to be done to utilize this system. If desired,

144     the entire setup can be easily placed in a standard 37°C, 5% CO2, humidified tissue culture

145     incubator. The peristaltic pump we adapted (Flocel [31]) has 4 pressure heads. When doing live

146     imaging, stage top space constraints use of all 4 pumps in tandem. Therefore, we often use the

147     system in a standard incubator to allow conversion of 2 pressure heads to carry laminar flow,

148     while two remain pulsatile to optimize throughput and pair culture conditions within a single

149     experiment. At the end of the experiment, the cells can be collected for biochemical/molecular

150     analysis to determine the downstream molecular impacts of individual flow stimuli: i.e. rinsed with

151     1x PBS and fixed with 4% paraformaldehyde (PFA) for immunostaining applications (discussed

152     below), flushed with TRIZOL for mRNA collection, or lysed in sample buffer for protein collection

153     [28].

154

## 155     **Immunostaining of cultures following flow**

156     Using our method, following the termination of flow, alterations in protein localization, cellular

157     signaling, or mRNA composition, among other parameters, can be analyzed in order to interrogate

158     downstream signaling pathways that occur as a consequence of flow. Here, we will outline our

159     immunostaining protocol for the analysis of protein accumulation and localization in response to

160     flow forces.

161

162     After 24 hours of exposure to flow stimuli, the cultured ECs were rapidly rinsed twice with 3 mL

163     1x PBS by flushing the slides using a 3 mL syringe. The cells were fixed in 100 μL of 4%

164     paraformaldehyde (PFA) for at least 4 hours before starting the immunostaining protocol.

165    Following fixation, the PFA solution is removed from the slides and the cells rinsed three times

166    with ice cold 1x PBS. If desired, the cultures can then be incubated with 100 µL of 0.1% TritonX-

167    100 in 1x PBS (PBST) for 10 minutes at room temperature, to permeabilize the cells and stain for

168    intracellular proteins. Next, the cells are then incubated in 100 µL blocking buffer (1% BSA, 0.3M

169    glycine in 1x PBST) at room temperature for 1 hour. A primary antibody is chosen for the desired

170    protein of interest, and is diluted into 1% BSA/1x PBST for incubation overnight at 4°C. The next

171    morning, the primary antibody is removed, and the cells rinsed with 1x PBST three times to

172    decrease non-specific antibody binding. Secondary antibody is then added at a 1:2000 dilution in

173    1% BSA/1x PBST and the slides incubated for 1 hour at room temperature. Finally, HOECHST

174    dye is added at a 1:5000 dilution and incubated for 30 minutes at room temperature for staining

175    of DNA/nuclei. Three washes with PBST are done at the end of all of the steps to remove excess

176    antibody and decrease non-specific background staining prior to mounting the slides for imaging

177    analysis. Images were acquired utilizing a 20x objective on a Nikon Ti2 inverted microscope.

178

179    As an example (**Fig 4**), the endothelial cell junctional protein VE-Cadherin was labeled (1:100

180    dilution of primary antibody) and visualized using an Alexa Fluro-488 secondary antibody (1:2000

181    dilution, green). Nuclei (HOECHST) labeling is in blue. As shown, application of flow forces across

182    endothelial cells enhances the accumulation of VE-Cadherin protein at junctions compared to no

183    flow controls (**Fig 4A**). While, no differences were noted in immunostaining intensity between

184    laminar and pulsatile flow conditions, marked differences in localization of the VE-Cadherin

185    protein were noted (**Fig 4B-E**).

186

## Discussion

188    In this work we outline the validation and use of a peristaltic pump system that can be easily

189    modified to concurrently deliver laminar or pulsatile flow to adjacent endothelial cell cultures in a

8

190   highly reproducible manner. The system provides a cost-effective, easy to use alternative for labs

191   looking to conduct *in vitro* flow modeling experiments. Additionally, the platform allows for real

192   time imaging of cellular responses to flow and analysis of behaviors (**Fig 3**), and following

193   exposure to flow forces, the cells can be utilized for molecular analysis [28] (**Fig 4**).

194

195   As part of this work, we compared the endogenous function of the peristaltic pump against our

196   lab-built pulse dampeners and a commercial pulse dampener (**Fig 2**). These studies

197   demonstrated the ability of our lab-built dampeners to generate laminar type flow as compared to

198   the pulsatile nature of the endogenous pump function. Additionally, our dampeners showed

199   improved performance for generation of laminar, non-pulsatile flow forces versus the commercial

200   dampener we tested. The analysis also confirms that our custom-built dampeners are stable

201   across at least 24 hours of assay at the temperature and humidity recommended for endothelial

202   cell culture (**Fig 2C,F,I**), showing that this system is suitable for use in functional assays.

203   Therefore, modification of a peristaltic pump to include dampeners into the system allows for an

204   affordable and adaptable method to culture cells under laminar and/or pulsatile flow conditions

205   for the reproducible study of shear stress mediated cellular responses *in vitro*.

206

207   Functionally, the peristaltic pump utilized has 4 pressure heads, allowing for side by side

208   comparison of cellular behavior under pulsatile versus laminar flow conditions. As shown by

209   cellular tracking experiments, cells under pulsatile flow move haphazardly and tend to end up

210   oriented perpendicular to the direction of flow (**Fig 3A-C,E; Video 3**), while cells under laminar

211   flow rapidly orient parallel to and move against the direction of flow (**Fig 3A,B,D,E, Video 4**).

212   These phenotypes are consistent with those published *in vitro* and *in vivo* under developmental

213   and non-pathogenic flow settings [5, 6, 13-16, 19, 20, 22-27, 29, 31, 33-38], suggesting that this

214   system is able to generate physiologically relevant flow forces. Finally, we confirm that endothelial

215   cells experiencing flow forces develop stronger junctions, as assessed by increased VE-Cadherin

9

216    localization at junctions compared to no flow conditions (**Fig 4**). While the intensity in staining is

217    not significantly different between cells experiencing pulsatile versus laminar flow, localization of

218    the protein at the junction is differentially oriented (**Fig 4C-E**). Similar results were described

219    previously in ECs cultures, where disturbed flow regions in a flow chamber exhibited

220    discontinuous VE-Cadherin staining, while in areas where the flow was laminar the VE-Cadherin

221    staining was continuous [39].

222

223    Being able to reliably model physiological flow conditions allows for deeper mechanistic study of

224    EC autonomous biology; however, it also opens up the possibility of identifying flow regulated

225    signals generated in ECs that alter physiology in a non-autonomous fashion. Embryonic and fetal

226    hematopoietic stem cells (HSCs) and vascular mural cells (MCs) are two primary examples of this

227    phenomenon. HSC development is dependent on blood flow via cell-intrinsic NO signaling [40].

228    HSC development via the Yes-activated protein (YAP) is also dependent on the mechanical

229    forces of blood flow, as shown by Lundin et al. using induced pluripotent stem cells grown in

230    microfluidic culture devices [41]. Beyond initial specification, HSCs extravasate into circulation

231    and seed developmental niches where they complete their developmental program (reviewed by

232    Horton et al. [42]). During this process, the HSCs are exposed to multiple vascular environments

233    experiencing a variety of mechanical stresses; these stresses trigger signaling events in vascular

234    cells which may play a role in determining ultimate hematopoietic cell fate, among other

235    physiological processes. While there has been tremendous progress in understanding the effects

236    of extracellular forces on HSC differentiation, our understanding of how these forces interface

237    with the vascular niche to signal to HSCs traversing blood vessels has been limited by technical

238    challenges.

239

240    Similarly, we have recently shown that differential sensing of blood flow forces can alter mural cell

241    (MC) biology during development [43, 44]. Arteries are known to acquire much greater numbers

10

242   of MCs than veins across development, and elevated mechanical forces felt by the arterial

243   vasculature is predicted to be a key driver in this process. However, how these forces are sensed

244   by ECs and subsequently communicated to MCs is still an active area of investigation. The

245   transcription factor Klf2 is well known to play an essential role in vascular development in

246   response to forces generated by blood flow [35, 36, 45-53]. In zebrafish and mice, during early

247   vascular development the expression of *klf2a/*Klf2 is significantly higher in veins compared with

248   expression in the dorsal aorta (DA), where the blood flow is pulsatory due to the DAs direct

249   connection to the heart [34, 43, 44]. We recently demonstrated that in *klf2a* deficient zebrafish,

250   there is a significant increase in association of MCs to the CV compared to wildtype siblings,

251   suggesting that Klf2 might serve as a direct or indirect transcriptional repressor for MC recruitment

252   cues [43]. This is just one example of the natural anatomical adaptations that result as a response

253   to the different types of flow forces experienced by vasculature during development or in disease.

254   Therefore, the development of a low cost and easy to use device to model blood flow forces, such

255   as the one described in this manuscript, has the potential to greatly expand our understanding of

256   the physiological effects of EC intrinsic and extrinsic signaling events.

11

# Materials and Methods:

| Product | Vendor | Catalogue number |
|---|---|---|
| **Supplies required to assemble the dampeners and flow system** | | |
| Elbow Luer Connector Male | ibidi | 10802 |
| T-type connector | Nalgene | 6151-0125 |
| Traceable™ Silicone Pump Tubing | FisherBrand | 15-078271 |
| µ-Slide \| $^{0.4}$ Luer | ibidi | 80176 |
| Plastic Bonder | JBweld | 50133H |
| 10 mL Syringe Luer-Lok Tip | Becton Dickinson (BD) | 302995 |
| 3 mL Syringe | Becton Dickinson (BD) | 309656 |
| Thinwall Polypropylene Tubes | Beckman | 331372 |
| 30 mL HDPE Bottles | Nalgene | 2104-0001 |
| Peristaltic pump and controller software | Flocel | WPX1 |
| **Supplies required to evaluate effect of dampeners** | | |
| Qdot 655 ITK organic quantum dots | Invitrogen | Q217721MP |
| Liquid Flow Sensor | Sensirion | SLF3S-1300F |
| Liquid Flow Pulsation Damping Kit | Sensirion | 403-LFPDKIT |
| **Reagents for Immunostaining** | | |
| Paraformaldehyde | Sigma-Aldrich | P6148 |
| Triton X-100 | Sigma-Aldrich | T9284 |
| Bovine Serum Albumin (BSA) | Sigma-Aldrich | A7030 |
| Goat IgG- anti-hVE-Cadhering | R&D Systems | AF938 |
| Alexa Fluro-488 donkey anti-goat | Invitrogen | A11055 |
| Hoechst 34580 | Sigma-Aldrich | 63493 |
| **Supplies for Cell Culture** | | |
| HUVEC-XL, Human Umbilical Vein Endothelial Cells | Lonza | 001911027 |
| Gelatin Type B | Fisher Chemicals | G7-500 |
| 1x M199 | Gibco | 11043-023 |
| Heparin sodium salt | Sigma-Aldrich | H3393-50KU |
| Antibiotic-Antimycotic (100x) | Gibco | 15240-062 |
| Endothelial Cell Growth Supplement | EMD Milliopore | 02-102 |
| Fetal Bovine Serum (FBS) | Gibco | 16140-071 |

# Acknowledgments:

265 **Figures:**

Abello, et al., Figure 1
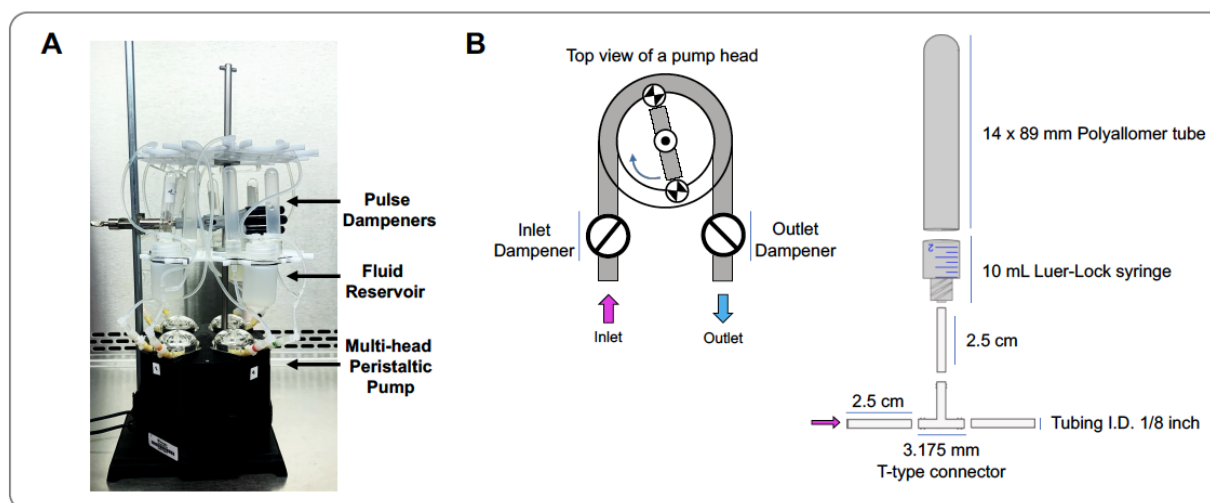


**Fig 1. Adaptations to a peristaltic pump to deliver laminar flow. A)** Picture of the flow system setup, including the 4 head peristaltic pump, dampeners, reservoirs, and slides. **B)** Left panel shows the schematic representation of a peristaltic pump' head including the positions of the dampeners. The right panel is a schematic representation of how to assemble the dampeners.

13

**Abello, et al., Figure 2**



274
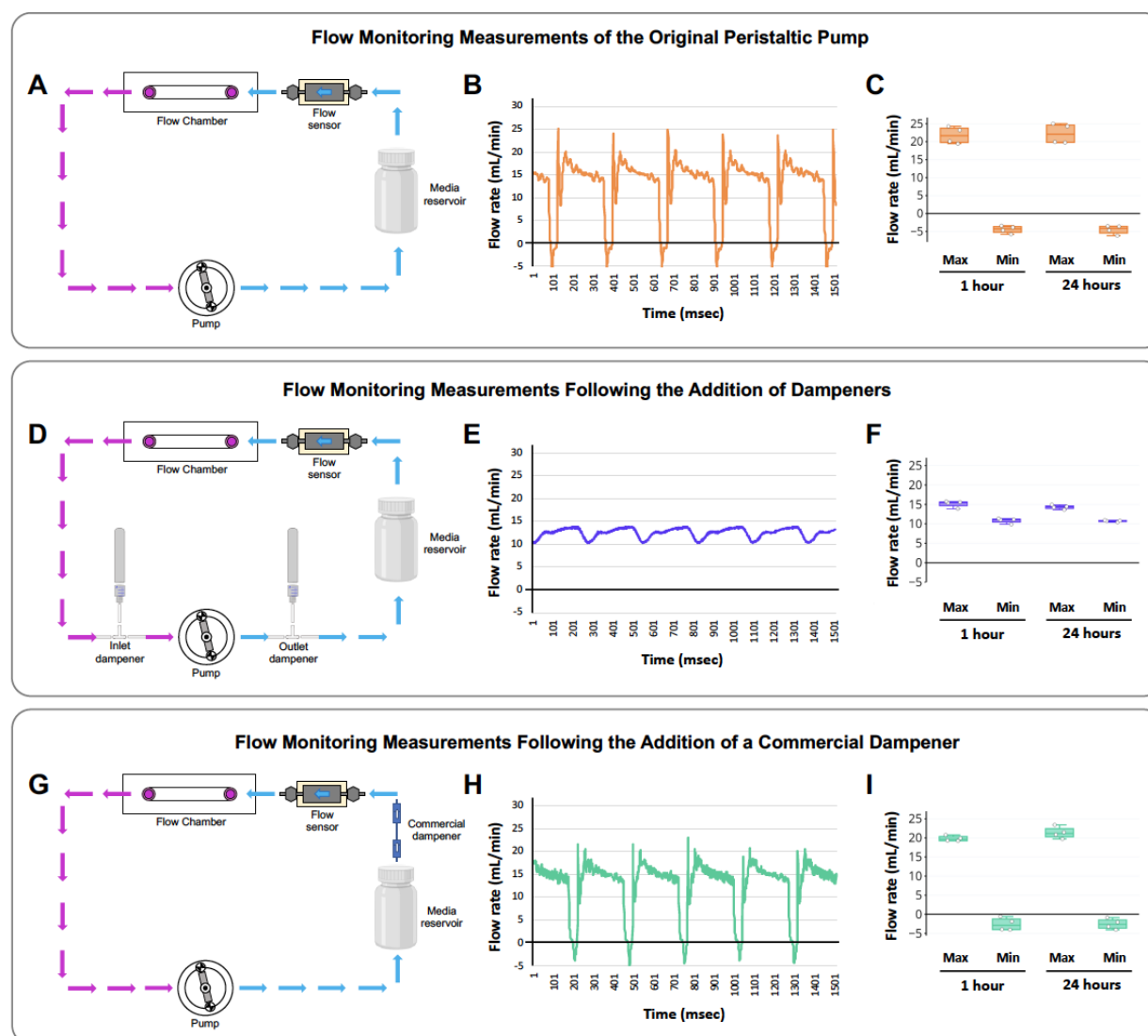
**Fig 2. Quantifying the effect of dampeners in off-setting pump pulsation.** A flow sensor was purchased to quantifiably measure the effects of dampeners in off-setting peristaltic pump pulsation. The flow sensor was placed directly prior to the flow chamber to ensure a representative measurement of flow forces felt by the endothelial cells in the culture. **A)** Schematic diagram of the flow circuit and placement of the flow sensor to measure flow forces generated by the original, non-modified peristaltic pump. **B)** Pulse traces collected across 1500 msec of pump function, demonstrating marked pulsation of the fluid that is being flowed across the endothelial cell monolayer. **C)** Average maximum and minimum flow forces generated by the endogenous

14

283   function of the peristaltic pump at 1 and 24 hours of culture. **D)** Schematic diagram of the modified

284   laminar flow circuit, including placement of our custom inlet/outlet dampeners and the flow sensor

285   to measure forces generated by off-setting the pulsation coming out of the peristaltic pump. **E)**

286   Pulse traces collected across 1500 msec of pump function, demonstrating laminar flow (i.e. 6-fold

287   suppression of fluid pulsation) across the endothelial cell monolayer. **F)** Average maximum and

288   minimum flow forces generated by the modified, laminar function of the peristaltic pump at 1 and

289   24 hours of culture. **G)** Schematic diagram of the modified laminar flow circuit, including

290   placement of a commercial dampener and the flow sensor to measure forces generated by off-

291   setting the pulsation coming out of the peristaltic pump. **H)** Pulse traces collected across 1500

292   msec of pump function, demonstrating mild suppression of fluid pulsation across the endothelial

293   cell monolayer. However, as shown, our dampeners suppressed pulsation to a much higher

294   degree (commercial 1.4-fold from peristaltic; lab-built 6-fold from peristaltic). **I)** Average maximum

295   and minimum flow forces generated after commercial dampener modifications of the peristaltic

296   pump at 1 and 24 hours of culture. The box plots are graphed showing the median versus the first

297   and third quartiles of the data (the middle, top, and bottom lines of the box respectively). The

298   whiskers demonstrate the spread of data within 1.5x above and below the interquartile range. All

299   data points (averages from individual pumps) are shown as discrete dots, with outliers shown

300   above or below the whiskers.

15

Abello, et al., Figure 3
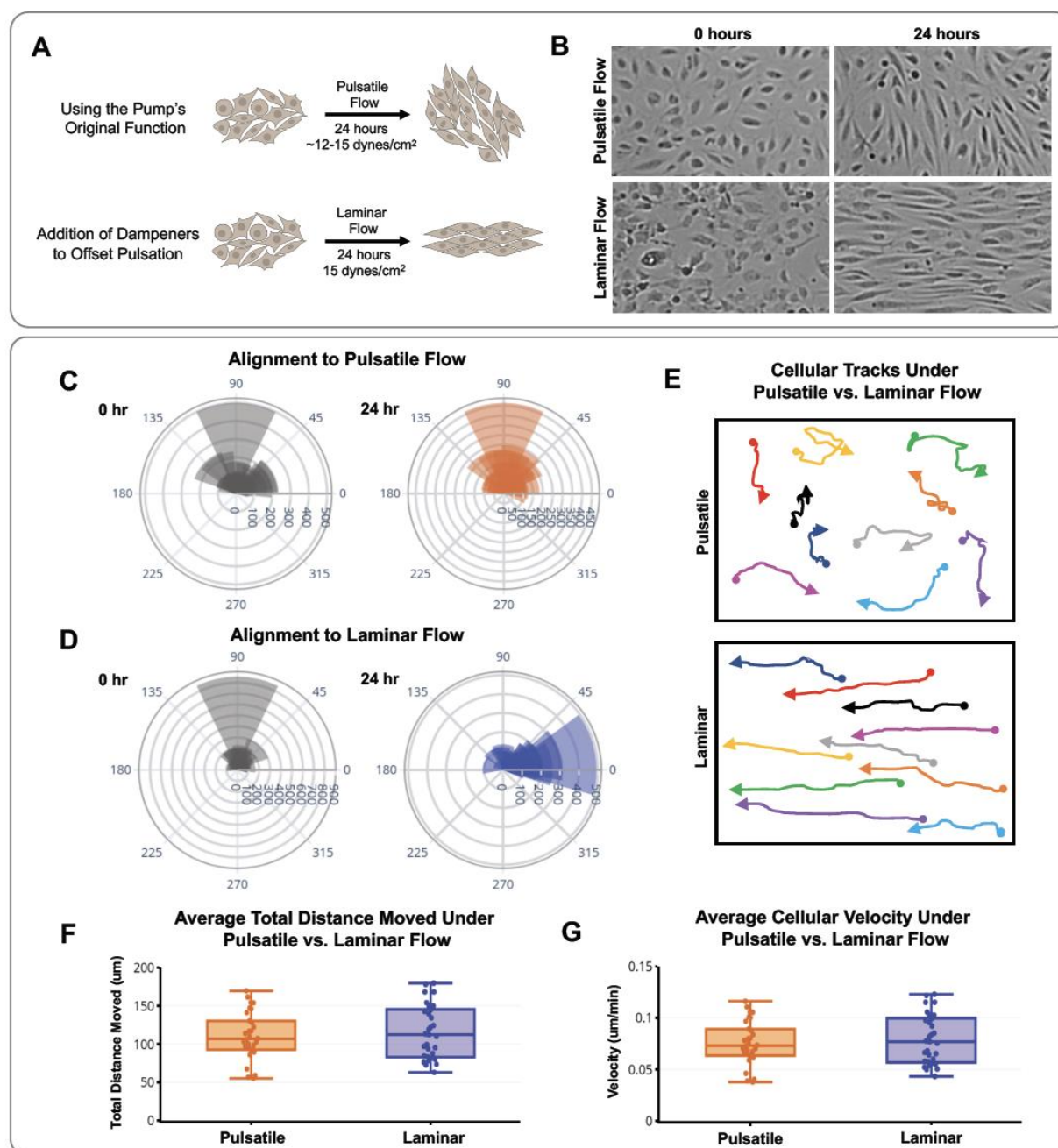


**Fig 3. Phenotypic characterization of pulsatile versus laminar flow conditions. A)** A cartoon of the cell alignment expected under pulsatile and laminar flow conditions (i.e. with and without dampeners). **B)** Microscopy images show HUVEC alignment under pulsatile versus laminar flow conditions at 0 and 24 hours as imaged utilizing our stage top incubated microscope system. **C,D)** Distribution angles of HUVECs, showing the orientation of the cell's longest axis relative to the

307    direction of flow at 0 hours (grey) and after 24 hours (orange/blue) of pulsatile (C) versus laminar

308    (D) flow. Cuboidal or symmetrical cells at 0 hours were measured as 90° to the direction of flow.

309    **E)** Representative cell tracks of HUVECs across the 24 hour period of pulsatile (top) or laminar

310    (bottom) flow. Arrow heads represents the direction of cellular movement, circles represent the

311    starting point of individual cells. **F,G)** Average distance traveled (F) and average velocity (G,

312    calculated based off of the average distance travelled over time) shown for pulsatile versus

313    laminar flow over the 24 hour period of treatment. The box plots are graphed showing the median

314    versus the first and third quartiles of the data (the middle, top, and bottom lines of the box

315    respectively). The whiskers demonstrate the spread of data within 1.5x above and below the

316    interquartile range. All data points (individual cells) are shown as discrete dots, with outliers shown

317    above or below the whiskers.

318

319

320

17

**Abello, et al., Figure 4**
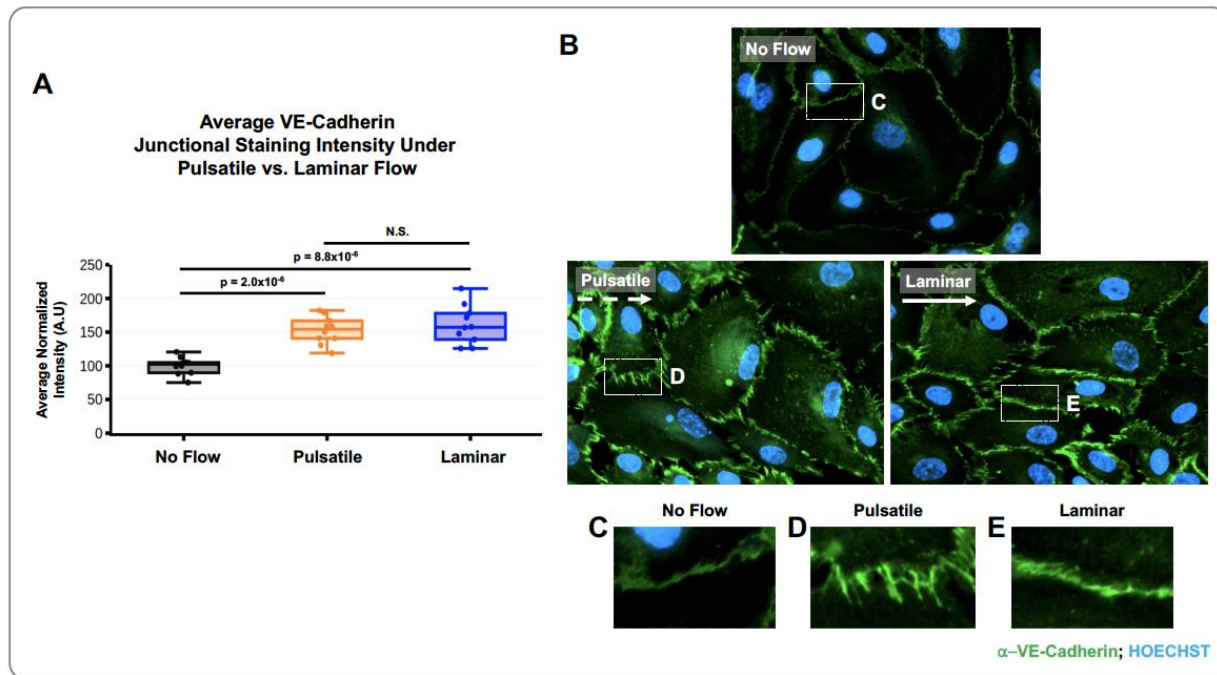


**Fig 4. Immunostaining the EC junctional marker, VE-Cadherin, under varying flow conditions**. **A)** Quantification of VE-Cadherin staining intensity at the endothelial cell junction. Black bar shows the no flow condition, orange bar shows staining intensity following exposure to pulsatile flow (original pump function), and the blue bar shows staining intensity following exposure to laminar flow (condition with dampeners). The box plots are graphed showing the median versus the first and third quartiles of the data (the middle, top, and bottom lines of the box respectively). The whiskers demonstrate the spread of data within 1.5x above and below the interquartile range. All data points (average intensity from individual images) are shown as individual dots, with outliers shown above or below the whiskers. p-values are indicated above statistically significant datasets and were generated using one-way ANOVA. **B)** Representative microscopy images of cells immunostained for VE-Cadherin (green) and nuclei (blue) under no flow, pulsatile flow, or laminar flow conditions. **C-E)** Zoomed in imaged of the white boxes shown in B, showing changes in localization and intensity of VE-Cadherin staining depending on flow forces applied to the endothelial cell monolayer.

18

# Supporting information

**Video 1. Visualization of Qdots under pulsatile flow conditions without dampeners.** Qdots were diluted 1:1000 in full culture media and flowed across the imaging slides for visualization in real-time. The video demonstrates Qdot movement under pulsatile flow conditions (the standard pump function without the pulse dampeners present) and a constant pump speed.

**Video 2. Visualization of Qdots under laminar flow conditions with dampeners.** Qdots were diluted 1:1000 in full culture media and flowed across the imaging slides for visualization in real-time. The video demonstrates Qdot movement with dampeners located at the inlet and outlet ports of the pump head to generate laminar flow at a constant pump speed.

**Video 3. Visualization of HUVECs under pulsatile flow conditions (without dampeners).** Human umbilical vein endothelial cells (HUVECs) were cultured on a μ-Slide | $^{0.4}$ Luer slide (2.5 x $10^5$ cell/slide) in full culture media. The video shows a 24 hour time lapse sequence, with images acquired at 20 minute intervals. The cells were cultured under pulsatile flow conditions (the standard pump function without the pulse dampeners present) and a constant pump speed.

**Video 4. Visualization of HUVECs under laminar flow conditions (utilizing dampeners).** Human umbilical vein endothelial cells (HUVECs) were cultured on a μ-Slide | $^{0.4}$ Luer slide (2.5 x $10^5$ cell/slide) in full culture media. The video shows a 24 hour time lapse sequence, with images acquired at 20 minute intervals. The cells were cultured under laminar flow conditions—i.e. dampeners located at the inlet and outlet ports of the pump head to generate laminar flow at a constant pump speed.

# References

1.  Menon NV, Su C, Pang KT, Phua ZJ, Tay HM, Dalan R, et al. Recapitulating atherogenic flow disturbances and vascular inflammation in a perfusable 3D stenosis model. Biofabrication. 2020;12(4):045009. Epub 2020/07/11. doi: 10.1088/1758-5090/aba501. PubMed PMID: 32650321.

2.  Terrell JA, Jones CG, Kabandana GKM, Chen C. From cells-on-a-chip to organs-on-a-chip: scaffolding materials for 3D cell culture in microfluidics. J Mater Chem B. 2020;8(31):6667-85. Epub 2020/06/23. doi: 10.1039/d0tb00718h. PubMed PMID: 32567628.

3.  Maurya MR, Gupta S, Li JY, Ajami NE, Chen ZB, Shyy JY, et al. Longitudinal shear stress response in human endothelial cells to atheroprone and atheroprotective conditions. Proc Natl Acad Sci U S A. 2021;118(4). Epub 2021/01/21. doi: 10.1073/pnas.2023236118. PubMed PMID: 33468662; PubMed Central PMCID: PMCPMC7848718.

4.  Swain SM, Liddle RA. Piezo1 acts upstream of TRPV4 to induce pathological changes in endothelial cells due to shear stress. J Biol Chem. 2021;296:100171. Epub 2020/12/11. doi: 10.1074/jbc.RA120.015059. PubMed PMID: 33298523; PubMed Central PMCID: PMCPMC7948745.

5.  Guo D, Chien S, Shyy JY. Regulation of endothelial cell cycle by laminar versus oscillatory flow: distinct modes of interactions of AMP-activated protein kinase and Akt pathways. Circ Res. 2007;100(4):564-71. Epub 2007/02/03. doi: 10.1161/01.RES.0000259561.23876.c5. PubMed PMID: 17272808.

6.  Eskin SG, Ives CL, McIntire LV, Navarro LT. Response of cultured endothelial cells to steady flow. Microvasc Res. 1984;28(1):87-94. Epub 1984/07/01. doi: 10.1016/0026-2862(84)90031-1. PubMed PMID: 6748961.

7.  Hu YL, Li S, Miao H, Tsou TC, del Pozo MA, Chien S. Roles of microtubule dynamics and small GTPase Rac in endothelial cell migration and lamellipodium formation under flow. J Vasc Res. 2002;39(6):465-76. Epub 2003/02/05. doi: 10.1159/000067202. PubMed PMID: 12566972.

8.  LaMack JA, Friedman MH. Individual and combined effects of shear stress magnitude and spatial gradient on endothelial cell gene expression. Am J Physiol Heart Circ Physiol. 2007;293(5):H2853-9. Epub 2007/09/04. doi: 10.1152/ajpheart.00244.2007. PubMed PMID: 17766484.

390    9.  Malek AM, Izumo S. Control of endothelial cell gene expression by flow. J Biomech.
391        1995;28(12):1515-28. Epub 1995/12/01. doi: 10.1016/0021-9290(95)00099-2. PubMed
392        PMID: 8666591.

393    10. Shiu YT, Li S, Marganski WA, Usami S, Schwartz MA, Wang YL, et al. Rho mediates the
394        shear-enhancement of endothelial cell migration and traction force generation. Biophys J.
395        2004;86(4):2558-65. Epub 2004/03/26. doi: 10.1016/S0006-3495(04)74311-8. PubMed
396        PMID: 15041692; PubMed Central PMCID: PMCPMC1304103.

397    11. Wang S, Tarbell JM. Effect of fluid flow on smooth muscle cells in a 3-dimensional collagen
398        gel model. Arterioscler Thromb Vasc Biol. 2000;20(10):2220-5. Epub 2000/10/14. doi:
399        10.1161/01.atv.20.10.2220. PubMed PMID: 11031207.

400    12. Ziegler T, Nerem RM. Effect of flow on the process of endothelial cell division. Arterioscler
401        Thromb. 1994;14(4):636-43. Epub 1994/04/01. doi: 10.1161/01.atv.14.4.636. PubMed PMID:
402        8148361.

403    13. Fang JS, Coon BG, Gillis N, Chen Z, Qiu J, Chittenden TW, et al. Shear-induced Notch-
404        Cx37-p27 axis arrests endothelial cell cycle to enable arterial specification. Nat Commun.
405        2017;8(1):2149. Epub 2017/12/17. doi: 10.1038/s41467-017-01742-7. PubMed PMID:
406        29247167; PubMed Central PMCID: PMCPMC5732288.

407    14. Wang C, Lu H, Schwartz MA. A novel in vitro flow system for changing flow direction on
408        endothelial cells. J Biomech. 2012;45(7):1212-8. Epub 2012/03/06. doi:
409        10.1016/j.jbiomech.2012.01.045. PubMed PMID: 22386042; PubMed Central PMCID:
410        PMCPMC3327813.

411    15. Miao H, Hu YL, Shiu YT, Yuan S, Zhao Y, Kaunas R, et al. Effects of flow patterns on the
412        localization and expression of VE-cadherin at vascular endothelial cell junctions: in vivo and
413        in vitro investigations. J Vasc Res. 2005;42(1):77-89. Epub 2005/01/08. doi:
414        10.1159/000083094. PubMed PMID: 15637443.

415    16. Liu Z, Ruter DL, Quigley K, Tanke NT, Jiang Y, Bautch VL. Single-Cell RNA Sequencing
416        Reveals Endothelial Cell Transcriptome Heterogeneity Under Homeostatic Laminar Flow.
417        Arterioscler Thromb Vasc Biol. 2021;41(10):2575-84. Epub 2021/08/27. doi:
418        10.1161/ATVBAHA.121.316797. PubMed PMID: 34433297; PubMed Central PMCID:
419        PMCPMC8454496.

420    17. Vion AC, Perovic T, Petit C, Hollfinger I, Bartels-Klein E, Frampton E, et al. Endothelial Cell
421        Orientation and Polarity Are Controlled by Shear Stress and VEGF Through Distinct
422        Signaling Pathways. Front Physiol. 2020;11:623769. Epub 2021/03/20. doi:

423    10.3389/fphys.2020.623769. PubMed PMID: 33737879; PubMed Central PMCID:
424    PMCPMC7960671.

425  18.  Steward R, Jr., Tambe D, Hardin CC, Krishnan R, Fredberg JJ. Fluid shear, intercellular
426    stress, and endothelial cell alignment. Am J Physiol Cell Physiol. 2015;308(8):C657-64. Epub
427    2015/02/06. doi: 10.1152/ajpcell.00363.2014. PubMed PMID: 25652451; PubMed Central
428    PMCID: PMCPMC4398851.

429  19.  Helmlinger G, Geiger RV, Schreck S, Nerem RM. Effects of pulsatile flow on cultured
430    vascular endothelial cell morphology. J Biomech Eng. 1991;113(2):123-31. Epub
431    1991/05/01. doi: 10.1115/1.2891226. PubMed PMID: 1875686.

432  20.  Dekker RJ, van Soest S, Fontijn RD, Salamanca S, de Groot PG, VanBavel E, et al.
433    Prolonged fluid shear stress induces a distinct set of endothelial cell genes, most specifically
434    lung Kruppel-like factor (KLF2). Blood. 2002;100(5):1689-98. Epub 2002/08/15. doi:
435    10.1182/blood-2002-01-0046. PubMed PMID: 12176889.

436  21.  Kataoka N, Ujita S, Sato M. Effect of flow direction on the morphological responses of
437    cultured bovine aortic endothelial cells. Med Biol Eng Comput. 1998;36(1):122-8. Epub
438    1998/06/06. doi: 10.1007/BF02522869. PubMed PMID: 9614760.

439  22.  Mohammed M, Thurgood P, Gilliam C, Nguyen N, Pirogova E, Peter K, et al. Studying the
440    Response of Aortic Endothelial Cells under Pulsatile Flow Using a Compact Microfluidic
441    System. Anal Chem. 2019;91(18):12077-84. Epub 2019/08/14. doi:
442    10.1021/acs.analchem.9b03247. PubMed PMID: 31407572.

443  23.  Simmers MB, Pryor AW, Blackman BR. Arterial shear stress regulates endothelial cell-
444    directed migration, polarity, and morphology in confluent monolayers. Am J Physiol Heart
445    Circ Physiol. 2007;293(3):H1937-46. Epub 2007/06/26. doi: 10.1152/ajpheart.00534.2007.
446    PubMed PMID: 17586613.

447  24.  Tovar-Lopez F, Thurgood P, Gilliam C, Nguyen N, Pirogova E, Khoshmanesh K, et al. A
448    Microfluidic System for Studying the Effects of Disturbed Flow on Endothelial Cells. Front
449    Bioeng Biotechnol. 2019;7:81. Epub 2019/05/22. doi: 10.3389/fbioe.2019.00081. PubMed
450    PMID: 31111027; PubMed Central PMCID: PMCPMC6499196.

451  25.  Young EW, Simmons CA. Macro- and microscale fluid flow systems for endothelial cell
452    biology. Lab Chip. 2010;10(2):143-60. Epub 2010/01/13. doi: 10.1039/b913390a. PubMed
453    PMID: 20066241.

454  26.  Poduri A, Chang AH, Raftrey B, Rhee S, Van M, Red-Horse K. Endothelial cells respond to
455    the direction of mechanical stimuli through SMAD signaling to regulate coronary artery size.

456    Development. 2017;144(18):3241-52. Epub 2017/08/02. doi: 10.1242/dev.150904. PubMed

457    PMID: 28760815; PubMed Central PMCID: PMCPMC5612251.

458    27. Flaherty JT, Pierce JE, Ferrans VJ, Patel DJ, Tucker WK, Fry DL. Endothelial nuclear

459    patterns in the canine arterial tree with particular reference to hemodynamic events. Circ

460    Res. 1972;30(1):23-33. Epub 1972/01/01. doi: 10.1161/01.res.30.1.23. PubMed PMID:

461    5007525.

462    28. Alghanem AF, Abello J, Maurer JM, Kumar A, Ta CM, Gunasekar SK, et al. The SWELL1-

463    LRRC8 complex regulates endothelial AKT-eNOS signaling and vascular function. Elife.

464    2021;10. Epub 2021/02/26. doi: 10.7554/eLife.61313. PubMed PMID: 33629656; PubMed

465    Central PMCID: PMCPMC7997661.

466    29. Coon BG, Baeyens N, Han J, Budatha M, Ross TD, Fang JS, et al. Intramembrane binding

467    of VE-cadherin to VEGFR2 and VEGFR3 assembles the endothelial mechanosensory

468    complex. J Cell Biol. 2015;208(7):975-86. Epub 2015/03/25. doi: 10.1083/jcb.201408103.

469    PubMed PMID: 25800053; PubMed Central PMCID: PMCPMC4384728.

470    30. Pech S, Richter R, Lienig J, editors. Peristaltic Pump with Continuous Flow and

471    Programmable Flow Pulsation. 2020 IEEE 8th Electronics System-Integration Technology

472    Conference (ESTC); 2020 15-18 Sept. 2020.

473    31. Cucullo L, Hossain M, Tierney W, Janigro D. A new dynamic in vitro modular capillaries-

474    venules modular system: cerebrovascular physiology in a box. BMC Neurosci. 2013;14:18.

475    Epub 2013/02/08. doi: 10.1186/1471-2202-14-18. PubMed PMID: 23388041; PubMed

476    Central PMCID: PMCPMC3598202.

477    32. Schindelin J, Arganda-Carreras I, Frise E, Kaynig V, Longair M, Pietzsch T, et al. Fiji: an

478    open-source platform for biological-image analysis. Nat Methods. 2012;9(7):676-82. Epub

479    2012/06/30. doi: 10.1038/nmeth.2019. PubMed PMID: 22743772; PubMed Central PMCID:

480    PMCPMC3855844.

481    33. Himburg HA, Dowd SE, Friedman MH. Frequency-dependent response of the vascular

482    endothelium to pulsatile shear stress. Am J Physiol Heart Circ Physiol. 2007;293(1):H645-

483    53. Epub 2007/02/27. doi: 10.1152/ajpheart.01087.2006. PubMed PMID: 17322417.

484    34. Sugden WW, Meissner R, Aegerter-Wilmsen T, Tsaryk R, Leonard EV, Bussmann J, et al.

485    Endoglin controls blood vessel diameter through endothelial cell shape changes in response

486    to haemodynamic cues. Nat Cell Biol. 2017;19(6):653-65. Epub 2017/05/23. doi:

487    10.1038/ncb3528. PubMed PMID: 28530658; PubMed Central PMCID: PMCPMC5455977.

488    35. Boon RA, Leyen TA, Fontijn RD, Fledderus JO, Baggen JM, Volger OL, et al. KLF2-induced

489    actin shear fibers control both alignment to flow and JNK signaling in vascular endothelium.

490  Blood. 2010;115(12):2533-42. Epub 2009/12/25. doi: 10.1182/blood-2009-06-228726.
491  PubMed PMID: 20032497.

492  36. Chu HR, Sun YC, Gao Y, Guan XM, Yan H, Cui XD, et al. Function of Kruppellike factor 2 in
493  the shear stressinduced cell differentiation of endothelial progenitor cells to endothelial cells.
494  Mol Med Rep. 2019;19(3):1739-46. Epub 2019/01/11. doi: 10.3892/mmr.2019.9819.
495  PubMed PMID: 30628700.

496  37. dela Paz NG, Walshe TE, Leach LL, Saint-Geniez M, D'Amore PA. Role of shear-stress-
497  induced VEGF expression in endothelial cell survival. J Cell Sci. 2012;125(Pt 4):831-43.
498  Epub 2012/03/09. doi: 10.1242/jcs.084301. PubMed PMID: 22399811; PubMed Central
499  PMCID: PMCPMC3311927.

500  38. Groenendijk BC, Van der Heiden K, Hierck BP, Poelmann RE. The role of shear stress on
501  ET-1, KLF2, and NOS-3 expression in the developing cardiovascular system of chicken
502  embryos in a venous ligation model. Physiology (Bethesda). 2007;22:380-9. Epub
503  2007/12/13. doi: 10.1152/physiol.00023.2007. PubMed PMID: 18073411.

504  39. Chien S. Effects of disturbed flow on endothelial cells. Annals of Biomedical Engineering.
505  2008;36(4):554-62. doi: 10.1007/s10439-007-9426-3. PubMed PMID:
506  WOS:000254176000006.

507  40. North TE, Goessling W, Peeters M, Li P, Ceol C, Lord AM, et al. Hematopoietic stem cell
508  development is dependent on blood flow. Cell. 2009;137(4):736-48. Epub 2009/05/20. doi:
509  10.1016/j.cell.2009.04.023. PubMed PMID: 19450519; PubMed Central PMCID:
510  PMCPMC2722870.

511  41. Lundin V, Sugden WW, Theodore LN, Sousa PM, Han A, Chou S, et al. YAP Regulates
512  Hematopoietic Stem Cell Formation in Response to the Biomechanical Forces of Blood Flow.
513  Dev Cell. 2020;52(4):446-60 e5. Epub 2020/02/08. doi: 10.1016/j.devcel.2020.01.006.
514  PubMed PMID: 32032546; PubMed Central PMCID: PMCPMC7398148.

515  42. Horton PD, Dumbali SP, Bhanu KR, Diaz MF, Wenzel PL. Biomechanical Regulation of
516  Hematopoietic Stem Cells in the Developing Embryo. Curr Tissue Microenviron Rep.
517  2021;2(1):1-15. Epub 2021/05/04. doi: 10.1007/s43152-020-00027-4. PubMed PMID:
518  33937868; PubMed Central PMCID: PMCPMC8087251.

519  43. Stratman AN, Burns MC, Farrelly OM, Davis AE, Li W, Pham VN, et al. Chemokine mediated
520  signalling within arteries promotes vascular smooth muscle cell recruitment. Commun Biol.
521  2020;3(1):734. Epub 2020/12/06. doi: 10.1038/s42003-020-01462-7. PubMed PMID:
522  33277595; PubMed Central PMCID: PMCPMC7719186.

523   44. Stratman AN, Pezoa SA, Farrelly OM, Castranova D, Dye LE, 3rd, Butler MG, et al.
524       Interactions between mural cells and endothelial cells stabilize the developing zebrafish
525       dorsal aorta. Development. 2017;144(1):115-27. Epub 2016/12/04. doi:
526       10.1242/dev.143131. PubMed PMID: 27913637; PubMed Central PMCID:
527       PMCPMC5278630.

528   45. Atkins GB, Jain MK. Role of Kruppel-like transcription factors in endothelial biology. Circ Res.
529       2007;100(12):1686-95. Epub 2007/06/23. doi: 10.1161/01.RES.0000267856.00713.0a.
530       PubMed PMID: 17585076.

531   46. Bhattacharya R, Senbanerjee S, Lin Z, Mir S, Hamik A, Wang P, et al. Inhibition of vascular
532       permeability factor/vascular endothelial growth factor-mediated angiogenesis by the Kruppel-
533       like factor KLF2. J Biol Chem. 2005;280(32):28848-51. Epub 2005/06/28. doi:
534       10.1074/jbc.C500200200. PubMed PMID: 15980434.

535   47. Chiplunkar AR, Curtis BC, Eades GL, Kane MS, Fox SJ, Haar JL, et al. The Kruppel-like
536       factor 2 and Kruppel-like factor 4 genes interact to maintain endothelial integrity in mouse
537       embryonic vasculogenesis. BMC Dev Biol. 2013;13:40. Epub 2013/11/23. doi:
538       10.1186/1471-213X-13-40. PubMed PMID: 24261709; PubMed Central PMCID:
539       PMCPMC4222490.

540   48. Dekker RJ, van Thienen JV, Rohlena J, de Jager SC, Elderkamp YW, Seppen J, et al.
541       Endothelial KLF2 links local arterial shear stress levels to the expression of vascular tone-
542       regulating genes. Am J Pathol. 2005;167(2):609-18. Epub 2005/07/29. doi: 10.1016/S0002-
543       9440(10)63002-7. PubMed PMID: 16049344; PubMed Central PMCID: PMCPMC1603569.

544   49. Lee JS, Yu Q, Shin JT, Sebzda E, Bertozzi C, Chen M, et al. Klf2 is an essential regulator of
545       vascular hemodynamic forces in vivo. Dev Cell. 2006;11(6):845-57. Epub 2006/12/05. doi:
546       10.1016/j.devcel.2006.09.006. PubMed PMID: 17141159.

547   50. Lin Z, Natesan V, Shi H, Dong F, Kawanami D, Mahabeleshwar GH, et al. Kruppel-like factor
548       2 regulates endothelial barrier function. Arterioscler Thromb Vasc Biol. 2010;30(10):1952-9.
549       Epub 2010/07/24. doi: 10.1161/ATVBAHA.110.211474. PubMed PMID: 20651277; PubMed
550       Central PMCID: PMCPMC3095948.

551   51. Parmar KM, Larman HB, Dai G, Zhang Y, Wang ET, Moorthy SN, et al. Integration of flow-
552       dependent endothelial phenotypes by Kruppel-like factor 2. J Clin Invest. 2006;116(1):49-58.
553       Epub 2005/12/13. doi: 10.1172/JCI24787. PubMed PMID: 16341264; PubMed Central
554       PMCID: PMCPMC1307560.

555   52. Sangwung P, Zhou G, Nayak L, Chan ER, Kumar S, Kang DW, et al. KLF2 and KLF4 control
556       endothelial identity and vascular integrity. JCI Insight. 2017;2(4):e91700. Epub 2017/02/28.

557    doi: 10.1172/jci.insight.91700. PubMed PMID: 28239661; PubMed Central PMCID:
558    PMCPMC5313061 exists.
559  53. Zhou Z, Tang AT, Wong WY, Bamezai S, Goddard LM, Shenkar R, et al. Cerebral cavernous
560    malformations arise from endothelial gain of MEKK3-KLF2/4 signalling. Nature.
561    2016;532(7597):122-6. Epub 2016/03/31. doi: 10.1038/nature17178. PubMed PMID:
562    27027284; PubMed Central PMCID: PMCPMC4864035.
563